DOI: 10.1002/ejic.201001138

# DNA Photocleavage and Cytotoxic Properties of Ferrocene Conjugates

**Basudev Maity,[a] Balabhadrapatruni V. S. K. Chakravarthi,[b] Mithun Roy,[a] Anjali A. Karande,[b][‡] and Akhil R. Chakravarty*[a]**

**Keywords:** Metallocenes / Iron / DNA cleavage / Cytotoxicity / Photodynamic therapy

Ferrocenyl conjugates 2-ferrocenylimidazophenanthroline (**1**) and 2-ferrocenylimidazophenanthrene (**2**) were prepared, characterized, and their photoinduced DNA cleavage and photocytotoxic activity were studied. 2-Phenylimidazophenanthroline (**3**) was used as a control species. Compound **2** was characterized by X-ray crystallography. The interaction of the compounds with double-stranded calf thymus DNA (CT DNA) was studied. The compounds show good binding affinity to CT DNA with $K_b$ values of approximately $10^5$ $M^{-1}$. Thermal denaturation data suggest the groove binding nature of the compounds. The redox-active compounds show poor chemical nuclease activity in the presence of hydrogen peroxide and glutathione (GSH). Compound **1** exhibits significant DNA photocleavage activity in visible light of 476 and 532 nm. Compound **3** shows only moderate DNA cleavage activity. The positive effect of the ferrocenyl moiety is demonstrated by the DNA photocleavage data. Mechanistic investigations reveal the formation of superoxide as well as hydroxyl radicals as the active species. The photocytotoxicity of the compounds in HeLa cells was studied upon irradiation with visible light (400–700 nm). Compound **1** shows efficient photocytotoxic activity with an $IC_{50}$ value of 13 μM, while compounds **2** and **3** are less active with $IC_{50}$ values of >50 and 22 μM, respectively.

## Introduction

Ferrocene and its conjugates are of importance in medicinal chemistry for their potential utility as bioorganometallic agents.[1–3] The interest in ferrocene is due to its excellent stability in biological media, its lipophilicity, and redox activity. Although ferrocene as such does not show any anticancer property, the one-electron oxidized ferrocenium ion is cytotoxic.[4,5] Ferrocene conjugates having different organic moieties have been studied for their medicinal properties. The examples of such conjugates include ferrocifen (ferrocene-appended tamoxifen) as anticancer agent and ferroquine (ferrocene-conjugated chloroquine) as antimalarial drug.[6–8] It has been observed that the substitution of the beta phenyl ring of hydroxytamoxifen by nontoxic ferrocene not only enhances its activity but also makes it strongly active towards hormone-independent breast cancer.[6] The cytotoxicity of various other ferrocene conjugates has been reported.[9–12] The ferrocenium ion has been found to be primarily responsible for the anticancer activity of these ferrocene conjugates. Ferrocene conjugates having organic chromophores that are capable of generating ferrocenium species upon photoactivation could be of importance as bioorganometallic agents in the photodynamic therapy (PDT) of cancer.[13–16]

The concept of using hitherto unknown bioorganometallic species as potential PDT agents originates from the successful use of porphyrin and phthalocyanine bases as photochemotherapeutic agents to treat cancer in a noninvasive method in which the cancer cells are selectively photoexposed to visible light to generate singlet oxygen as the reactive oxygen species, thus leaving the unexposed healthy cells unaffected.[17–20] Metal-based PDT agents that show significant photocytotoxicity with reduced dark toxicity have recently been reported as alternatives to organic PDT agents.[21–30] We have recently shown that ferrocene-appended copper(II) complexes incorporating the photoactive dipyridoquinoxaline or dipyridophenazine bases in their structure are efficient photocleavers of plasmid DNA under red light.[31–33] The present work stems from our continued effort to design new photoactive ferrocene conjugates as bioorganometallics that are capable of showing photoinduced DNA cleavage activity and photocytotoxicity under visible light. We studied two ferrocene conjugates, **1** and **2**, having the ferrocenyl moiety linked to the respective imidazophenanthroline and imidazophenanthrene moiety (Figure 1). Herein, we present the DNA binding, DNA photocleavage activity, and photocytotoxicity in HeLa cells of these compounds. To explore the effect of the ferrocenyl moiety on the DNA cleavage activity, we prepared the phenyl analogue 2-phenylimidazophenanthroline (**3**) as a control species. Compound **2** has been characterized by X-

[a] Department of Inorganic and Physical Chemistry, Indian Institute of Science,
Bangalore 560012, India
Fax: +91-80-23600683
E-mail: arc@ipc.iisc.ernet.in
[b] Department of Biochemistry, Indian Institute of Science,
Bangalore 560012, India
[‡] Corresponding author for cellular studies
Supporting information for this article is available on the WWW under http://dx.doi.org/10.1002/ejic.201001138.

  

ray crystallography. The significant results of this study include the PDT effect observed for the 2-ferrocenylimidazophenanthroline conjugate in visible light. Interestingly, the mechanistic pathway observed for the DNA cleavage reactions of 2-ferrocenylimidazophenanthroline is different from that known for the organic PDT agents.[34,35]

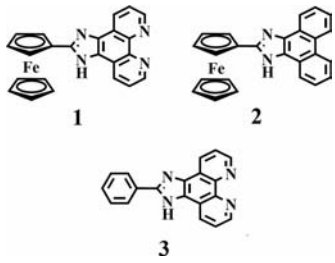


Figure 1. The ferrocene conjugates **1**, **2**, and the control species **3** used.

## Results and Discussion

### Synthesis and General Aspects

Compounds **1** and **3** were prepared by following literature procedures.[36,37] Compound **2** was synthesized in good yield by heating ferrocene-2-carboxaldehyde, phenanthrene-9,10-dione, and ammonium acetate at reflux. The compounds were characterized by spectroscopic and analytical methods. Selected physicochemical data are given in Table 1. The NMR spectra of compounds **1** and **3** are in accordance with the reported literature values.[36,37] The prominent molecular ion peak in the ESI-MS study indicates the stability of the compounds. The solution stability of the compounds has also been studied by electronic spectroscopy. The spectra of the compounds in 1:1 aqueous DMF, monitored for 8 h in the dark, did not show any apparent change. The molar conductivity data in DMF at 25 °C indicate the nonconducting nature of the compounds. The electronic spectrum of compound **2** showed a ferrocenyl band at 443 nm (Figure 2).[13] Compound **1**, which is very similar to compound **2**, showed three transitions at 430, 480, and 528 nm as shoulders assignable to the charge-transfer transitions involving the ferrocenyl and phenanthroline moieties. Compound **3**, which lacks the ferrocenyl moiety, did not show any visible spectral band.

Table 1. Selected physicochemical data and DNA binding parameters for **1**–**3**.

| Compd. | $\lambda_{max}$ /nm ($\varepsilon$ /dm$^3$ M$^{-1}$ cm$^{-1}$)[a] | $E_f$ /V ($\Delta E_p$ /mV)[b] | $K_b$[c] /M$^{-1}$ | $\Delta T_m$[d] /°C |
|---|---|---|---|---|
| **1** | 430, 480, 528[e] | 0.59 (95) | $1.3(\pm0.3) \times 10^5$ | 1.2 |
| **2** | 443 (830) | 0.52 (90) | $1.8(\pm0.4) \times 10^5$ | 1.9 |
| **3** | – | – | $2.4(\pm0.6) \times 10^5$ | 1.8 |

[a] In aqueous DMF (4:1 v/v). [b] The $Fc^+$/Fc redox couple in DMF (0.1 M KCl), $E_f = 0.5(E_{pa} + E_{pc})$, $\Delta E_p = (E_{pa} - E_{pc})$, where $E_{pa}$ and $E_{pc}$ are the anodic and cathodic peak potential, respectively. Potentials are vs. SCE. Scan rate: 100 mV S$^{-1}$. [c] Intrinsic equilibrium DNA binding constant from UV/Vis titration experiment. [d] Change in CT DNA melting temperature. [e] Shoulders having $\varepsilon$ values of 1110, 840, and 520 dm$^3$ M$^{-1}$ cm$^{-1}$, respectively.

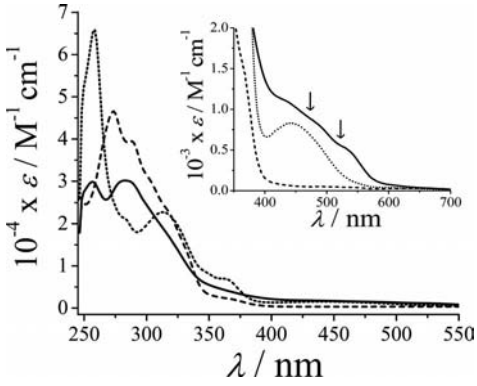


Figure 2. Electronic absorption spectra of **1** (−), **2** (···), and **3** (---) in aqueous DMF (1:4 v/v). The arrows indicate the wavelengths of laser light used for photoinduced DNA cleavage studies.

The compounds are redox-active in DMF (0.1 M TBAP), showing quasi-reversible cyclic voltammetric response near 0.55 V vs. SCE. The higher potential of **1** and **2** relative to that of ferrocene ($E_f$ = 0.42 V) indicates the higher redox stability of the conjugates in DMF. An anodic shift of the $Fc^+$/Fc redox potential could be due to the electron-withdrawing nature of the imidazophenanthroline or imidazophenanthrene moiety. Compound **3**, which lacks the ferrocenyl moiety, showed only two reduction responses near –1.59 and –1.86 V. Compound **1** showed similar reduction responses near –1.65 and –1.93 V. Interestingly, the ferrocenylimidazophenanthrene compound **2** did not show any reductive responses. The reduction responses in **1** and **3** could be due to the presence of two phenanthroline nitrogen atoms and not due to the imidazole moiety.

### X-ray Crystallography

Compound **2** was structurally characterized by single-crystal X-ray diffraction. The compound crystallizes in the $C222_1$ space group of the orthorhombic crystal system. Two cyclopentadienyl rings of the ferrocenyl unit are in an eclipsed conformation. A perspective view of the molecule is shown in Figure 3, and selected bond lengths are given in Table 2. The dihedral angle between two cyclopentadienyl rings is only 0.38°, indicating that the two rings are essentially parallel to each other. The plane containing the imidazophenanthrene ring forms dihedral angles of 4.16° and 4.53° with the cyclopentadienyl rings containing atoms C1 to C5 and C6 to C10. The iron atom is slightly displaced towards the cyclopentadienyl ring containing the imidazophenanthrene ring, which results in a Fe···Cp [C6–C10] ring centroid distance of 1.646 Å, whereas the other Fe···Cp [C1–C5] ring centroid distance is 1.663 Å. The Fe–C distances are in the range 2.034 to 2.046 Å with an average value of 2.041 Å. A partial π–π stacking interaction is observed between the imidazophenanthrene ring and free cyclopentadienyl ring of another molecule.

  

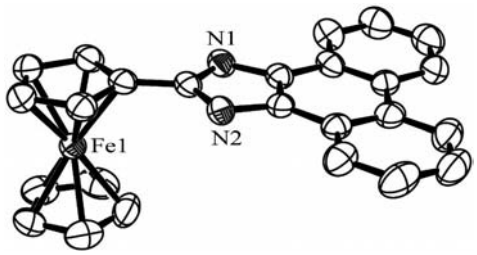


Figure 3. An ORTEP view of compound **2** showing 50% probability thermal ellipsoids and the atom numbering scheme for the metal and hetero atoms. The hydrogen atoms are not shown for clarity.

Table 2. Selected bond lengths (in Å) for compound **2**.

| | | | |
|---|---|---|---|
| Fe1–C1 | 2.035(4) | Fe1–C6 | 2.040(3) |
| Fe1–C2 | 2.040(4) | Fe1–C7 | 2.044(3) |
| Fe1–C3 | 2.046(6) | Fe1–C8 | 2.034(3) |
| Fe1–C4 | 2.045(3) | Fe1–C9 | 2.040(6) |
| Fe1–C5 | 2.040(4) | Fe1–C10 | 2.046(3) |
| Fe1–$C_0^1$[a] | 1.646 | Fe1–$C_0^2$[b] | 1.663 |

[a] $C_0^1$ is the centroid of the cyclopentadienyl ring containing atoms C6 to C10. [b] $C_0^2$ is the centroid of the cyclopentadienyl ring containing atoms C1 to C5.

## DNA Binding Studies

The interaction of the compounds with double-stranded calf thymus DNA was studied by UV/Vis absorption titration and thermal denaturation. The intrinsic binding constants of compounds **1**–**3** to DNA were obtained by the absorption titration method, giving $K_b$ values in the range $1.3 \times 10^5$ to $2.4 \times 10^5$ $M^{-1}$ in the order: **3** > **2** ≥ **1** (Figure 4). An intercalative mode of DNA binding generally leads to a significant change in absorbance with hypochromism and redshift of the band due to stacking of the aromatic chromophore between the DNA base pairs.[38] The groove binding or electrostatic interaction results in only moderate spectral changes. The electronic absorption spectra of the compounds in 15% DMF-Tris-HCl buffer medium (pH 7.2) showed only moderate hypochromicity (ca. 20%), indicating the groove binding propensity of the compounds. DNA binding by the compounds was also studied by the thermal denaturation method. The change in the DNA melting temperature varied from 1.2 to 1.8 °C, while the DNA intercalator ethidium bromide gave a significantly higher $\Delta T_m$ value of 8.1 °C under similar conditions. The DNA melting data suggest groove binding and/or partial intercalative binding of compounds **1**–**3** to CT DNA (Table 1).[39]

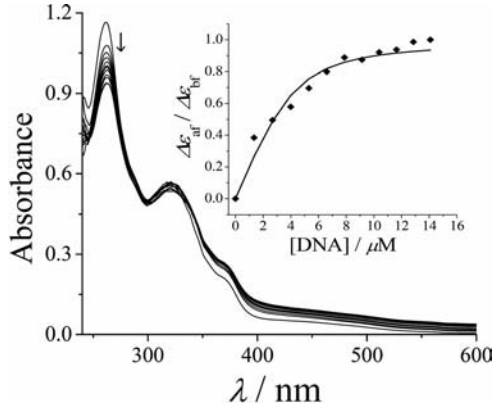


Figure 4. Spectral traces showing the effect of gradual addition of CT DNA (270 μM NP) to a 20 μM solution of compound **2** in DMF-Tris-HCl buffer medium. The inset shows the plot of $\Delta\varepsilon_{af}/\Delta\varepsilon_{bf}$ vs. [DNA].

## DNA Cleavage Activity

The oxidative cleavage of SC pUC19 DNA (0.2 μg, 30 μM) by the compounds was studied in the presence of the cellular reducing agent glutathione in its reduced form and hydrogen peroxide as oxidizing agent.[40] Compounds **1** and **2** showed poor chemical nuclease activity in the presence of hydrogen peroxide (0.1 mM). This could be due to higher $E_f$ values of the conjugates relative to that of ferrocene. Compound **3**, which lacks the ferrocenyl moiety, is inactive in the presence of hydrogen peroxide. The ferrocene conjugates did not show any chemical nuclease activity in the presence of glutathione.

The photocleavage activity of the compounds was studied by using SC pUC19 DNA upon irradiation with UV-A light of 365 nm and laser light of different visible wavelengths [476 (blue light), 532 (green light), and 647 nm (red light)] (Figure 5). The DNA photocleavage activity follows the order: **1** >> **3** > **2**. Selected DNA photocleavage data are given in Table 3. An 8 μM solution of compound **1** showed essentially complete cleavage of DNA to its nicked circular form in UV-A light. Compound **1** also showed significant DNA cleavage activity in blue or green light and relatively less activity in red light. Compound **3**, which lacked the ferrocenyl moiety, showed lower DNA photocleavage activity. Compound **2**, having the ferrocenyl moiety, did not show any significant DNA photocleavage activity. The results suggest the importance of the photoactive phenanthroline moiety having two nitrogen atoms that could undergo n–π* transitions for the presence of DNA photocleavage activity.[41] The compounds are inactive in the dark, which excludes the possibility of DNA hydrolysis. Inactivity of the compounds under an argon atmosphere indicates the necessity for molecular oxygen to generate reactive oxygen species (ROS) to photocleave DNA.

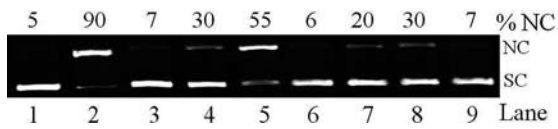


Figure 5. Gel electrophoresis diagram showing the visible-light-induced DNA cleavage activity of **1**–**3** (20 μM) with SC pUC19 DNA (0.2 μg, 30 μM b.p.) for an exposure time of 2 h. Lane 1: DNA control (476 nm); lane 2: DNA + **1** (476 nm); lane 3: DNA + **2** (476 nm); lane 4: DNA + **3** (476 nm); lane 5: DNA + **1** (532 nm); lane 6: DNA + **2** (532 nm); lane 7: DNA + **3** (532 nm); lane 8: DNA + **1** (647 nm); lane 9: DNA + **3** (647 nm).

  

Table 3. Selected SC pUC19 DNA (0.2 μg, 30 μM b.p.) photocleavage data for **1**–**3**.

| Reaction conditions | $\lambda$[a] /nm | %NC[b] |
|---|---|---|
| DNA control | 365 | 4 |
| DNA + **1** | 365 | 92 |
| | 476 | 90 |
| | 532 | 55 |
| | 647 | 30 |
| DNA + **2** | 365 | 17 |
| | 476 | 7 |
| | 532 | 6 |
| DNA + **3** | 365 | 25 |
| | 476 | 30 |
| | 532 | 20 |
| | 647 | 7 |

[a] Wavelength used for DNA photocleavage reactions. Compound concentration is 8 μM for 365 nm and 20 μM for visible light experiments. Exposure time: 2 h. [b] NC is the nicked circular form of supercoiled pUC19 DNA.

The mechanistic aspects of the DNA photocleavage reactions were studied by radical quenching experiments with external additives (Figure 6). Superoxide radical scavenger SOD or hydroxyl radical scavenger potassium iodide and catalase inhibited the DNA photocleavage activity of compound **1**, indicating the formation $O_2^{\cdot-}$ and $HO^{\cdot}$ species in the reaction medium. No apparent change in the DNA cleavage activity was observed in the presence of singlet oxygen quenchers like TEMP or DABCO. The mechanistic data suggest a photoredox pathway, involving the ferrocenyl moiety, in which $O_2^{\cdot-}$ and $HO^{\cdot}$ species are formed.[42] In contrast, DNA photocleavage by compound **3** proceeds by a type-II mechanistic pathway, showing significant inhibition with singlet oxygen quenchers and no inhibition in the presence of hydroxyl radical scavengers.

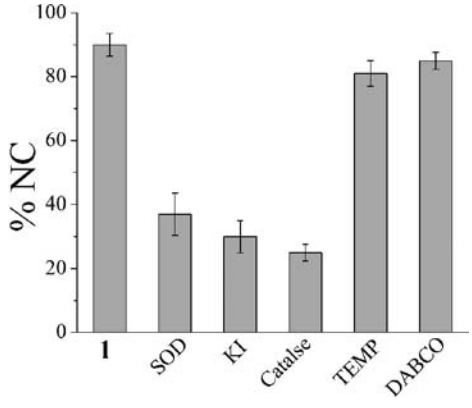


Figure 6. Bar diagram showing the photoinduced pUC19 DNA (0.2 μg, 30 μM b.p.) cleavage activity of compound **1** (20 μM) in the presence of different singlet oxygen quenchers and hydroxyl radical scavengers at 476 nm for an exposure time of 2 h [concentrations of the additives: DABCO, TEMP, KI: 1 mM; catalase and SOD: 8 units].

UV photolysis experiments were carried out with compound **1**, which showed three shoulders at 430, 480, and 527 nm in aqueous DMF. Upon irradiation with UV-A light of 365 nm, two peaks at 490 and 532 nm gradually appeared. Similarly, when the compound was treated with an oxidizing agent like ammonium ceric(IV) nitrate, similar bands at 490 and 527 nm were obtained. In the dark, there was no apparent change in the visible spectral pattern for up to 8 h. The results indicate that compound **1** could undergo oxidation at the ferrocenyl moiety and the oxidized species could lead to the degradation of DNA.[31]

## Photocytotoxicity Study

The cytotoxicity of the compounds on the human cervical carcinoma HeLa cell line was evaluated. Since the compounds showed limited aqueous solubility, the concentration was limited to 50 μM. The $IC_{50}$ values were obtained from the MTT assay (Figure 7). Compounds **1** and **3** showed significant cytotoxicity to HeLa cells with $IC_{50}$ values of 33 and 38 μM, respectively, in the dark, whereas compound **2** did not show cytotoxicity, with an $IC_{50}$ value of >50 μM. The cytotoxicity of **1** and **3** was found to increase on irradiation with visible light of 400–700 nm. The enhancement of cytotoxicity was greater for compound **1** having a conjugated ferrocenyl moiety, reaching an $IC_{50}$ value of 13 μM. The phenyl analogue, compound **3**, showed relatively lower photocytotoxicity, giving an $IC_{50}$ value of 22 μM. The ferrocenyl moiety in **1** seems to be responsible for its higher photocytotoxicity, which is in agreement with the greater enhancement of the DNA photocleavage activity of **1** relative to that of **3**. The activity of compound **1** is lower when compared to Photofrin®, the FDA-approved PDT drug, having reported $IC_{50}$ values of 4.3 μM in red light and >41 μM in the dark.[43] The anticancer drug cisplatin did not show any PDT effect and its $IC_{50}$ value is significantly higher than that of Photofrin® in red light for HeLa cells.[44]

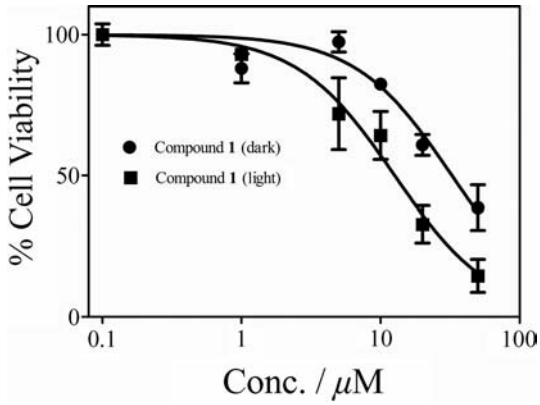


Figure 7. Cytotoxicity of compound **1** in human cervical HeLa cancer cells upon incubation for 4 h in the dark followed by irradiation by visible light (400 to 700 nm) as determined by MTT assay. The cells treated in the dark and the photoexposed cells are shown by circles and squares, respectively.

## PDT Effect on Nuclear Morphology

Hoechst staining was performed to understand the mode of cell death induced by compound **1** upon photoexcitation

  

with visible light. The change in the nuclear morphology could indicate the cell death mechanism. To identify the possible involvement of apoptosis, the visible-light-irradiated HeLa cells treated with compound **1** (15 μM for 4 h in the dark) were stained with Hoechst 33258 stain. A significant increase in the apoptotic nuclear morphology such as extensive chromatin aggregation or nuclear condensation was evidenced by shrinkage in cell volume and membrane blebbing in the treated cells as compared to the evenly stained nuclear contours of the normal or untreated HeLa cells, suggesting apoptosis (Figure 8).[45,46] The PDT effect of **1** is evidenced from significant increase in the population of apoptotic nuclei upon irradiation of the HeLa cells in the presence of **1**.

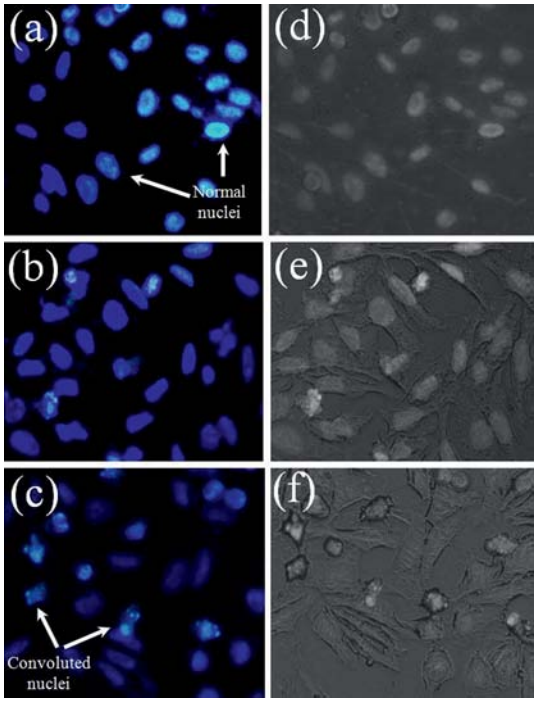


Figure 8. Panels (a) to (c) show Hoechst 33258 staining of compound **1** (15 μM) in untreated and treated HeLa cells permeabilized with TBST and fixed with paraformaldehyde (3.7%), 1 h after photoexposure to identify nuclear morphology: (a) untreated cells, (b) cells treated with compound **1** kept in the dark, and (c) cells treated with compound **1** and exposed to visible light (10 $J\,cm^{-2}$). Panels (d) to (f) are the corresponding bright field images.

## Conclusions

We studied two ferrocene conjugates, and the one having the imidazophenanthroline moiety shows significant photoinduced pUC19 DNA cleavage activity in visible light and photocytotoxicity in visible light in HeLa cells. The compounds show binding propensity to calf thymus DNA. Interestingly, the conjugate having the imidazophenanthrene moiety does not show any DNA photocleavage activity and photocytotoxicity. Complex **1** forms the superoxide anion radical and hydroxyl radical species in the DNA photocleavage reactions. The mechanistic pathway is thus different from that known for common organic PDT agents, involving the formation of singlet oxygen as the reactive species. The PDT effect observed for compound **1** is significant, since the use of bioorganometallic compounds in PDT is virtually unknown in the literature. Ferrocene, being a less cytotoxic molecule, provides an opportunity to develop bioorganometallic compounds as photochemotherapeutic agents by suitable design of the stable conjugate species having biologically important photoactive moieties with potential anticancer properties, as exemplified by ferrocifen.

## Experimental Section

**Materials:** The reagents and chemicals were purchased from commercial sources. Ferrocene-2-carboxaldehyde, calf thymus DNA, agarose (molecular biology grade), catalase, superoxide dismutase, TEMP (2,2,6,6-tetramethyl-4-piperidone), DABCO (1,4-diazabicyclo[2.2.2]octane), and ethidium bromide (EB) were purchased from Sigma–Aldrich (USA). The supercoiled (SC) pUC19 DNA (cesium chloride purified) was procured from Bangalore Genie (India). Tris(hydroxymethyl)aminomethane-HCl (Tris-HCl) and phosphate buffer were prepared by using doubly distilled water. The solvents were purified by standard procedures.[47] Compounds **1** and **3** were prepared by following literature procedures.[36,37]

**Measurements:** The NMR spectra were recorded with a Bruker Avance 400 (400 MHz) NMR spectrometer. The elemental analyses were performed by using a thermo Finnigan FLASH EA 1112 CHNS analyzer. Mass spectra were obtained with a Bruker Esquire 300 Plus ESI (Bruker daltonics) spectrometer. The IR spectra of the solid samples were recorded with a Perkin–Elmer Lambda 35 instrument. The electronic absorption spectroscopic and DNA melting experiments were carried out by using Cary 300 bio UV/Vis spectrometer. Conductivity measurements were performed by using a Control Dynamics (India) conductivity meter. Cyclic voltammetric measurements were carried out at room temperature with an EG&G PAR 253 VersaStat potentiostat/galvanostat having a three electrode configuration consisting of a glassy carbon working, a platinum wire auxiliary, and a saturated calomel (SCE) reference electrode. Ferrocene ($E_f$ = 0.43 V) was used as standard in DMF containing 0.1 M tetrabutylammonium perchlorate (TBAP).

**Compound 2:** A mixture of phenanthrene-9,10-dione (0.26 g, 1.25 mmol), ammonium acetate (0.96 g, 12.5 mmol), ferrocene-2-carboxaldehyde (0.27 g, 1.25 mmol), and acetic acid (1 mL) in chloroform (25 mL) was heated at reflux with stirring for 10 h. After cooling, the solution was neutralized with a saturated aqueous $NaHCO_3$ solution, during which orange precipitation appeared, and the solid product was removed by filtration. The filtrate was then extracted with chloroform (3 × 25 mL). The combined organic layers were dried with $Na_2SO_4$ and filtered, and the filtrate, after concentration, gave an orange residue. The combined residue was recrystallized from $CH_2Cl_2$ (Yield = 0.40 g, ca. 70%). $C_{25}H_{18}FeN_2$ (402.26): calcd. C 74.64, H 4.51, N 6.96; found C 74.41, H 4.77, N 6.74. $^1H$ NMR (400 MHz, [D$_6$]DMSO): $\delta$ = 4.13 (s, 5 H), 4.48 (s, 2 H), 5.16 (s, 2 H), 7.59 (dd, $J$ = 7.6, 7.2 Hz, 2 H), 7.69 (dd, $J$ = 7.2, 7.2 Hz, 2 H), 8.50 (d, $J$ = 8.0 Hz, 2 H), 8.83 (d, $J$ = 8.0 Hz, 2 H), 13.18 (br., NH) ppm. ESI-MS (in MeCN): $m/z$ = 402 $[M]^+$. Molar conductance: $\Lambda_M$ = 21 $S\,m^2\,M^{-1}$ in aqueous DMF at 25 °C. IR (KBr phase): $\tilde{\nu}$ = 3382 (w, br.), 2835 (w), 1610 (m), 1564 (w), 1449 (m), 1413 (s), 1348 (m), 1233 (m), 1106 (w), 1037 (w), 999 (m), 971 (s), 819 (m), 759 (s), 728 (s), 510 (w) $cm^{-1}$. UV/Vis in

  

aqueous DMF (1:4): $\lambda_{max}$ ($\varepsilon$ [dm$^3$ M$^{-1}$cm$^{-1}$]) = 260 (65900), 284 sh (21200), 314 (22600), 367 (2170), 443 (830) nm.

**Solubility and Stability:** All the compounds were soluble in DMF, MeCN, and DMSO; they were moderately soluble in $CH_2Cl_2$ and MeOH. They were stable in the solid and solution (aqueous DMF or DMSO) phases in the dark.

**X-ray Crystallography:** Single crystals suitable for X-ray diffraction were grown by slow concentration of a dichloromethane solution of compound **2**. X-ray intensity data on the single crystal of **2** were measured by using a Bruker Smart Kappa APEX II CCD Detector with a fine-focused sealed tube with graphite-monochromated Mo-$K_\alpha$ ($\lambda$ = 0.71073 Å) radiation at 293 K using the $\omega$-scan mode. The molecular structure of **2** was solved by direct methods (SHELX-97), and all non-hydrogen atoms were refined anisotropically on $F^2$ using the full-matrix least-squares procedure.[48] Empirical absorption corrections were made by using the multi-scan program. All non-hydrogen atoms were refined with anisotropic thermal displacement parameters. All hydrogen atoms were added at their calculated positions and refined by using a riding model. The perspective view of the compound was obtained with ORTEP-3 for Windows.[49] Details of the crystallographic data collection and solution parameters are given in Table 4. CCDC-797006 contains the crystallographic data for this paper. These data can be obtained free of charge from The Cambridge Data Centre via www. ccdc.ac.uk/data-request/cif.

Table 4. Selected crystallographic data for compound **2**.

| | **2** |
|---|---|
| Chemical formula | $C_{25}H_{18}FeN_2$ |
| M /g mol$^{-1}$ | 402.26 |
| Crystal system | orthorhombic |
| Space group | $C222_1$ |
| *a* /Å | 9.7865(18) |
| *b* /Å | 19.247(4) |
| *c* /Å | 19.164(4) |
| *a*, *ß*, *γ* /° | 90.0 |
| *Z* | 8 |
| *T* /K | 293(2) |
| Volume /Å$^3$ | 3609.8(12) |
| D /g cm$^{-3}$ | 1.480 |
| $\mu$ (Mo-$K_\alpha$) /mm$^{-1}$ | 0.848 |
| $\theta$ min–max /° | 2.12–30.57 |
| *R*(int) | 0.0566 |
| *F*(000) | 1664 |
| GOF on $F^2$ | 0.954 |
| $R1[I > 2\sigma(I)]$ | 0.0486 |
| $wR2$[a] | 0.0787 |

[a] $w = [\sigma^2(F_o^2) + (0.0319P)^2 + 0.0000P]^{-1}$, where $P = [F_o^2 + 2F_c^2]/3$.

**DNA Binding Experiments:** The UV/Vis absorption titration and thermal denaturation techniques were used. The UV/Vis absorption titration was carried out by following a reported procedure in 5 mM Tris-HCl buffer medium (pH 7.2) containing 15% DMF by using CT DNA.[33,50] The concentration of the CT DNA was varied from 0 to 13 μM during the titration. The binding affinity of the compounds to DNA was evaluated from the intrinsic equilibrium binding constant ($K_b$) values.[51,52] Thermal denaturation experiments were carried out by following a published procedure in 5 mM phosphate buffer (pH 6.8)/NaCl medium containing 15% DMF.[53] The ratio of DNA to complex was 10:1. A control experiment was done by using ethidium bromide as a classical DNA intercalator.

**DNA Cleavage Experiments:** The cleavage of supercoiled (SC) pUC19 DNA (30 μM, 0.2 μg, 2686 base pairs) by the compounds was studied in 50 mM Tris-HCl/NaCl buffer (pH 7.2) by following a reported literature procedure.[33] The reactions were carried out with a UV-A lamp of 365 nm (6 W, sample area of illumination: 45 mm$^2$) and visible light using a CW Ar-Kr laser (100 mW, laser beam diameter = 1.8 mm, beam divergence = 0.7 mrad, Spectra Physics water-cooled mixed-gas ion laser Stabilite 2018-RM). The power of the laser beam was measured by using a Spectra Physics CW laser power meter (model 407A). All the samples were incubated at 37 °C for 45 min prior to photoexposure. For mechanistic investigations, TEMP and DABCO, as singlet oxygen quenchers, superoxide dismutase, as superoxide radical scavenger, and KI, catalase, and mannitol as hydroxyl radical scavengers, were used. The chemical nuclease reactions were carried out by incubating the samples in the presence of hydrogen peroxide (0.1 mM) as an oxidizing agent and glutathione (1 mM) as a reducing agent for 2 h at 37 °C in the dark. The extent of DNA cleavage was estimated by measuring the intensities of the bands with the UVITECH gel documentation system and by applying corrections for the low level of NC form present in the SC DNA sample and for the low affinity of EB binding to SC compared to the NC form of DNA.[54] The observed error in measuring the band intensities in the agarose gel was ca. 5%.

**MTT Assay and Hoechst Staining**

The cellular toxicity of the compounds was studied by using 3-(4,5-dimethylthiazol-2-yl)-2,5-diphenyltetrazolium bromide (MTT) assay based on the ability of mitochondrial dehydrogenases in the viable cells to cleave the tetrazolium rings of MTT, forming dark blue membrane-impermeable crystals of formazan that can be quantified at 595 nm on detergent solubilization. The amount of the formazan product formed gave a measure of the viable cells.[55] Approximately 10000 HeLa cells (human cervical carcinoma cell line) were placed in a 96-well culture plate in Dulbecco's modified Eagle's medium (DMEM) supplemented with 10% fetal bovine serum (FBS). The cells were incubated for 24 h at 37 °C in a $CO_2$ incubator, and then different concentrations of compounds **1**–**3** (1–50 μM) were added, and incubation was continued for another 4 h in the dark. The stock solution of the compounds, which was initially prepared in DMSO, was diluted with cell culture medium (DMEM) to make the final concentration of DMSO in the sample solution 1%. Prior to irradiation, the medium was replaced by PBS, and the cell plates were exposed to visible light (400–700 nm, Luzchem Photoreactor, light dose of 10 J cm$^{-2}$). After irradiation, PBS was replaced with DMEM supplemented with 10% FBS, and incubated for another 24 h in the dark followed by addition of MTT (20 μL of a 5 mg mL$^{-1}$ solution) and then incubated for additional 3 h. Finally, the culture medium was discarded, and DMSO (200 μL) was added to dissolve the formazan crystals. The absorbance of the formazan in DMSO solution was measured at 595 nm by using a BIORAD ELISA plate reader. The cytotoxicity of the test compound was measured as the percentage ratio of the absorbance of the treated cells to the untreated controls. The $IC_{50}$ values were determined by nonlinear regression analysis (Graph Pad Prism).

The changes in chromatin organization such as condensation of chromatin and nuclear fragmentations characteristic to apoptosis, following photoexposure after treatment with **1**, were determined microscopically by assessing staining with Hoechst 33258. Hoechst staining was performed as described by Lee and Shacter.[56] Briefly, the control and the cells treated with **1** (15 μM) for 4 h in the dark, followed by irradiation with visible light of 400–700 nm (10 J cm$^{-2}$), were fixed with 4% (v/v) paraformaldehyde in PBS for 10 min at room temperature, permeabilized with 0.1% Triton X-100 for

  

10 min, and stained with Hoechst 33258 (1 mg mL$^{-1}$ in PBS) for 5 min. After being washed twice with PBS, cells were examined by fluorescence microscopy (360/40 nm excitation and 460/50 nm emission filters). The apoptotic cells were identified by the presence of highly condensed or fragmented nuclei.[57]

**Supporting Information** (see footnote on the first page of this article): ESI-MS spectrum of **2**, $^1$H NMR spectrum, UV/Vis spectra, cyclic voltammograms, unit cell packing and π–π stacking interaction diagrams, UV/Vis binding plot, DNA melting plot, gel electrophoresis diagrams, photolysis diagram, and MTT plot for photocytotoxicity.

## Acknowledgments

We thank the Department of Science and Technology (DST), Government of India, for financial support [SR/S5/MBD-02/2007]. We are thankful to the DST for a CCD diffractometer facility and the Alexander von Humboldt Foundation, Germany, for the donation of an electroanalytical system. A. R. C. thanks the DST for a J. C. Bose national fellowship. We are thankful to Mr. Sounik Saha for his help in creating the cover page figure.

[1] C. G. Hartinger, P. J. Dyson, *Chem. Soc. Rev.* **2009**, *38*, 391–401.
[2] M. F. R. Fouda, M. M. Abd-Elzaher, R. A. Abdelsamaia, A. A. Labib, *Appl. Organomet. Chem.* **2007**, *21*, 613–625.
[3] D. R. Van Staveren, N. Metzler-Nolte, *Chem. Rev.* **2004**, *104*, 5931–5985.
[4] G. Tabbì, C. Cassino, G. Cavigiolio, D. Colangelo, A. Ghiglia, I. Viano, D. Osella, *J. Med. Chem.* **2002**, *45*, 5786–5796.
[5] D. Osella, M. Ferrali, P. Zanello, F. Laschi, M. Fontani, C. Nervi, G. Cavigiolio, *Inorg. Chim. Acta* **2000**, *306*, 42–48.
[6] G. Jaouen, S. Top, A. Vessires, G. Leclercq, M. J. McGlinchey, *Curr. Med. Chem.* **2004**, *11*, 2505–2517.
[7] A. Vessires, S. Top, P. Pigeon, E. Hillard, L. Boubeker, D. Spera, G. Jaouen, *J. Med. Chem.* **2005**, *48*, 3937–3940.
[8] C. Biot, *Curr. Med. Chem. Anti-Infect. Agents* **2004**, *3*, 135–147.
[9] J. C. Swarts, T. G. Vosloo, S. J. Cronje, W. C. Du Plessis, C. E. J. Van Rensburg, E. Kref, J. E. Vanlier, *Anticancer Res.* **2008**, *28*, 2781–2784.
[10] E. W. Neuse, F. Kanzawa, *Appl. Organomet. Chem.* **1990**, *4*, 19–26.
[11] A. J. Corry, A. Goel, S. R. Alley, P. N. Kelly, D. O'Sullivan, D. Savage, P. T. M. Kenny, *J. Organomet. Chem.* **2007**, *692*, 1405–1410.
[12] C. L. Ferreira, C. B. Ewart, C. A. Barta, S. Little, V. Yardley, C. Martins, E. Polishchuk, P. J. Smith, J. R. Moss, M. Merkel, M. J. Adam, C. Orvig, *Inorg. Chem.* **2006**, *45*, 8414–8422.
[13] S. Fery-Forgues, B. Delavaux-Nicot, *J. Photochem. Photobiol. A: Chem.* **2000**, *132*, 137–159.
[14] S. Fukuzumi, K. Okamoto, Y. Yoshida, H. Imahori, Y. Araki, O. Ito, *J. Am. Chem. Soc.* **2003**, *125*, 1007–1013.
[15] R. Martínez, I. Ratera, A. Tárraga, P. Molina, J. Veciana, *Chem. Commun.* **2006**, 3809–3811.
[16] E. M. McGale, B. H. Robinson, J. Simpson, *Organometallics* **2003**, *22*, 931–939.
[17] R. Bonnett, *Chemical Aspects of Photodynamic Therapy*, Gordon & Breach, London, U. K., **2000**.
[18] B. W. Henderson, T. M. Busch, L. A. Vaughan, N. P. Frawley, D. Babich, T. A. Sosa, J. D. Zollo, A. S. Dee, M. T. Cooper, D. A. Bellnier, W. R. Greco, A. R. Oseroff, *Cancer Res.* **2000**, *60*, 525–529.
[19] M. R. Detty, S. L. Gibson, S. J. Wagner, *J. Med. Chem.* **2004**, *47*, 3897–3915.
[20] D. E. G. J. Dolmans, D. Fukumura, R. K. Jain, *Nature Rev. Cancer* **2003**, *3*, 380–387.
[21] N. J. Farrer, L. Salassa, P. J. Sadler, *Dalton Trans.* **2009**, 10690–10701.
[22] M. J. Rose, N. L. Fry, R. Marlow, L. Hinck, P. K. Mascharak, *J. Am. Chem. Soc.* **2008**, *130*, 8834–8846.
[23] H. T. Chifotides, K. R. Dunbar, *Acc. Chem. Res.* **2005**, *38*, 146–156.
[24] A. M. Angeles-Boza, H. T. Chifotides, J. D. Aguirre, A. Chouai, P. K.-L. Fu, K. R. Dunbar, C. Turro, *J. Med. Chem.* **2006**, *49*, 6841–6847.
[25] U. Schatzschneider, *Eur. J. Inorg. Chem.* **2010**, 1451–1467.
[26] A. D. Ostrowski, P. C. Ford, *Dalton Trans.* **2009**, 10660–10669.
[27] K. Szacilowski, W. Macyk, A. Drzewiecka-Matuszek, M. Brindell, G. Stochel, *Chem. Rev.* **2005**, *105*, 2647–2694.
[28] D. Crespy, K. Landfester, U. S. Schubert, A. Schiller, *Chem. Commun.* **2010**, *46*, 6651–6662.
[29] P. K. Sasmal, S. Saha, R. Majumdar, R. R. Dighe, A. R. Chakravarty, *Chem. Commun.* **2009**, 1703–1705.
[30] S. Saha, R. Majumdar, M. Roy, R. R. Dighe, A. R. Chakravarty, *Inorg. Chem.* **2009**, *48*, 2652–2663.
[31] B. Maity, M. Roy, B. Banik, R. Majumdar, R. R. Dighe, A. R. Chakravarty, *Organometallics* **2010**, *29*, 3632–3641.
[32] T. K. Goswami, M. Roy, M. Nethaji, A. R. Chakravarty, *Organometallics* **2009**, *28*, 1992–1994.
[33] B. Maity, M. Roy, S. Saha, A. R. Chakravarty, *Organometallics* **2009**, *28*, 1495–1505.
[34] M. C. DeRosa, R. J. Crutchley, *Coord. Chem. Rev.* **2002**, *233–234*, 351–371.
[35] E. D. Sternberg, D. Dolphin, C. Brückner, *Tetrahedron* **1998**, *54*, 4151–4202.
[36] F. Zapata, A. Caballero, A. Espinosa, A. Tárraga, P. Molina, *J. Org. Chem.* **2008**, *73*, 4034–4044.
[37] N. M. Shavaleev, H. Adams, J. A. Weinstein, *Inorg. Chim. Acta* **2007**, *360*, 700–704.
[38] A. M. Pyle, J. P. Rehmann, R. Meshoyrer, C. V. Kumar, N. J. Turro, J. K. Barton, *J. Am. Chem. Soc.* **1989**, *111*, 3051–3058.
[39] G. A. Neyhart, N. Grover, S. R. Smith, W. A. Kalsbeck, T. A. Fairley, M. Cory, H. H. Thorp, *J. Am. Chem. Soc.* **1993**, *115*, 4423–4428.
[40] T. B. Thederahn, M. D. Kuwabara, T. A. Larsen, D. S. Sigman, *J. Am. Chem. Soc.* **1989**, *111*, 4941–4946.
[41] K. Toshima, R. Takano, T. Ozawa, S. Matsumura, *Chem. Commun.* **2002**, 212–213.
[42] C. J. Burrows, J. G. Muller, *Chem. Rev.* **1998**, *98*, 1109–1151.
[43] E. Delaey, F. Van Larr, F. De Vos, A. Kamuhabwa, P. Jacobs, P. de Witte, *J. Photochem. Photobiol. B: Biology* **2000**, *55*, 27–36.
[44] H. C. Kang, I.-J. Kim, H.-W. Park, S.-G. Jang, S.-A. Ahn, S. N. Yoon, W. J. Chang, B. C. Yoo, J.-G. Park, *Cancer Lett.* **2007**, *247*, 40–47.
[45] D. Ribble, N. B. Goldstein, D. A. Norris, Y. G. Shellman, *BMC Biotechnol.* **2005**, *5*, 12–18.
[46] C. Renvoize, A. Biola, M. Pallardy, J. Breard, *Cell Biol. Toxicol.* **1998**, *14*, 111–120.
[47] D. D. Perrin, W. L. F. Armarego, D. R. Perrin, *Purification of Laboratory Chemicals*, Pergamon Press, Oxford, **1980**.
[48] G. M. Sheldrick, *SHELX-97*, *Programs for Crystal Structure Solution and Refinement*, University of Göttingen, Göttingen, Germany.
[49] C. K. Johnson, *ORTEP-III, Report ORNL-5138*, Oak Ridge National Laboratory, Oak Ridge, TN, **1976**.
[50] M. E. Reichman, S. A. Rice, C. A. Thomas, P. Doty, *J. Am. Chem. Soc.* **1954**, *76*, 3047–3053.
[51] J. D. McGhee, P. H. Von Hippel, *J. Mol. Biol.* **1974**, *86*, 469–489.
[52] M. T. Carter, M. Rodriguez, A. J. Bard, *J. Am. Chem. Soc.* **1989**, *111*, 8901–8911.
[53] J. M. Kelly, A. B. Tossi, D. J. McConnell, C. OhUigin, *Nucl. Acid. Res.* **1985**, *13*, 6017–6034.
[54] J. Bernadou, G. Pratviel, F. Bennis, M. Girardet, B. Meunier, *Biochemistry* **1989**, *28*, 7268–7275.

  

[55] T. Mosmann, *J. Immunol. Methods* **1983**, *65*, 55–63.
[56] Y. J. Lee, E. Shacter, *J. Biol. Chem.* **1999**, *274*, 19792–19798.
[57] J. E. Coligan, A. M. Kruisbeck, D. H. Margulies, E. M. Shevach, W. Strober in *Related Isolation Procedures and Functional Assay, Current Protocols in Immunology* (Ed.: R. Coico), John Wiley & Sons, Inc., New York, **1995**, p. 3.17.1.

Received: October 25, 2010
Published Online: January 20, 2011

  